

Tilted fiber Bragg grating sensor interrogation system using a high-resolution silicon-on-insulator arrayed waveguide grating

Pavel Cheben,^{1,*} Edith Post,¹ Siegfried Janz,¹ Jacques Albert,² Albane Laronche,² Jens H. Schmid,¹ Dan-Xia Xu,¹ Boris Lamontagne,¹ Jean Lapointe,¹ André Delâge,¹ and Adam Densmore¹

¹*Institute for Microstructural Sciences, National Research Council Canada, 1200 Montreal Road, Building M50, Ottawa, Ontario K1A 0R6, Canada*

²*Department of Electronics, Carleton University, 1125 Colonel By Drive, Ottawa, Ontario K1S 5B6, Canada*

*Corresponding author: pavel.cheben@nrc.ca

Received July 16, 2008; revised September 5, 2008; accepted October 2, 2008;
posted October 9, 2008 (Doc. ID 98920); published November 12, 2008

We report a compact high-resolution arrayed waveguide grating (AWG) interrogator system designed to measure the relative wavelength spacing between two individual resonances of a tilted fiber Bragg grating (TFBG) refractometer. The TFBG refractometer benefits from an internal wavelength and power reference provided by the core mode reflection resonance that can be used to determine cladding mode perturbations with high accuracy. The AWG interrogator is a planar waveguide device fabricated on a silicon-on-insulator platform, having 50 channels with a 0.18 nm wavelength separation and a footprint of 8 mm × 8 mm. By overlaying two adjacent interference orders of the AWG we demonstrate simultaneous monitoring of two widely separated resonances in real time with high wavelength resolution. The standard deviation of the measured wavelength shifts is 1.2 pm, and it is limited by the resolution of the optical spectrum analyzer used for the interrogator calibration measurements. © 2008 Optical Society of America

OCIS codes: 280.4788, 120.6200, 130.3120, 130.7408, 350.2770.

The arrayed waveguide grating (AWG) [1–4] is a key device in wavelength division multiplexed (WDM) optical communication networks where it performs functions such as wavelength multiplexing and demultiplexing, wavelength filtering, signal routing, and optical cross-connects, among others. In recent years, AWGs have been increasingly used in areas other than WDM, including signal processing, spectral analysis, and sensing [4]. AWGs can be implemented with many wavelength channels and a high spectral resolution using high index contrast silicon-on-insulator (SOI) waveguides, since the large refractive index contrast between the silicon waveguide core ($n_{\text{Si}} \sim 3.5$) and the surrounding silica cladding ($n_{\text{SiO}_2} \sim 1.45$) ensures a very small device footprint [5,6].

Here we demonstrate an implementation of a highly sensitive interrogator for a fiber Bragg grating (FBG) refractometric sensor using our recently developed compact SOI AWG microspectrometer [6]. AWGs have been used for the interrogation of various types of FBG sensors [7–9]. In such experiments, the FBG resonance wavelength shifts induced by the measurand (e.g., stress, deformation, temperature, refractive index, etc.) are monitored by the AWG, which essentially performs the function of a spectrometer. However, the comparatively large channel spacing of previously reported AWG interrogators [8,9], typically 100 GHz (0.8 nm, at the wavelength $\lambda = 1.55 \mu\text{m}$), limits the minimum measurable wavelength shifts in the FBG spectrum. According to the AWG interrogator theory [10], by decreasing both the AWG channel passband and spacing by a factor of k , the wavelength resolution is increased by the same factor. In this Letter we demonstrate an SOI AWG with a channel spacing of 22.5 GHz and a 3 dB chan-

nel passband of 0.14 nm, the smallest values reported for an AWG interrogator (to our knowledge). With this device we demonstrate the real-time simultaneous measurement of cladding and Bragg mode resonances whose wavelength separation exceeds the free spectral range (FSR) of our AWG, achieving a wavelength resolution of ~ 1 pm and a negligible temperature cross sensitivity.

In the work presented here, the tilted fiber Bragg grating (TFBG), which was reported in detail in [11], was used to sense the refractive index of the medium surrounding the fiber. Tilting the grating plane enhances the coupling of the light from the forward propagating core mode to the backward propagating cladding modes. As a result, many resonance minima occur in the TFBG transmission spectrum. The fundamental Bragg resonance at wavelength $\lambda_B = 2n_{\text{core}}\Lambda$ corresponds to the coupling between the forward and backward propagating core modes. The cladding mode resonances are located at wavelengths $\lambda_{\text{clad},i} = (n_{\text{core}} + n_{\text{clad},i})\Lambda$, where n_{core} and $n_{\text{clad},i}$ are the core and cladding mode effective indices at specific resonance wavelengths and Λ is the projection of the grating period along the fiber axis. Since the cladding modes are guided by the cladding outer boundary, with the evanescent field in the surrounding medium, their effective indices depend on the refractive index of the medium. On the other hand, the effective index of the core mode is independent of the properties of the surrounding medium, since the core is isolated from the medium by the cladding. However the temperature sensitivities of both the core and cladding mode indices are nearly equal. Thus, by measuring the wavelength separation $\Delta(\lambda_B - \lambda_{\text{clad},i})$ between the Bragg and any one of the cladding resonances, refractive index changes can be monitored, while the

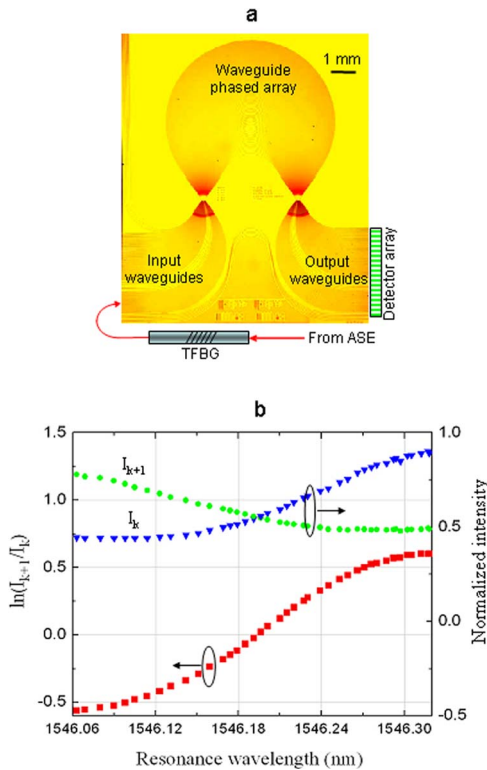


Fig. 1. (Color online) a, High-resolution SOI AWG sensor interrogator. Light from a broadband amplified spontaneous emission (ASE) source is coupled to a TFBG sensor. TFBG and cladding mode resonance wavelengths are measured by the AWG with the output waveguides coupled to a photodetector array. b, Light intensities and their logarithmic ratio for two adjacent AWG channels as a function of Bragg resonance wavelength shift.

influence of temperature fluctuations is minimized. The TFBG used in our experiment has a cross sensitivity of $\Delta(\lambda_B - \lambda_{\text{clad},i})$ to a temperature as small as $0.3 \text{ pm}/^\circ\text{C}$ [11].

We used our high-resolution SOI AWG spectrometer [6] as the interrogation circuit (Fig. 1a). The AWG has 50 output waveguides, each receiving a different wavelength channel, and the measured channel spacing is 0.18 nm (22.5 GHz at 1550 nm). We believe this is the densest spacing and the largest number of channels reported to date for an AWG of a comparable size [4], making this device particularly suitable for the FBG sensor interrogation. The measured FSR is 8.95 nm . The size advantage of our SOI AWG is also remarkable, as previously reported 25 GHz AWGs fabricated in glass waveguides occupy a 10 mm wafer, compared to the $8 \text{ mm} \times 8 \text{ mm}$ footprint of our microspectrometer.

Fiber grating resonances are measured by coupling the light transmitted through the grating into the AWG microspectrometer and monitoring the AWG output channel powers using a photodetector array, as shown in Fig. 1a. The wavelength shifts of the Bragg and of any cladding mode resonances λ_{res} are determined from the optical power in two adjacent AWG output channels with the TFBG resonance minima in between the two, i.e., $\lambda_k < \lambda_{\text{res}} < \lambda_{k+1}$. Figure 1b shows the variation in output power of two such AWG channels as the wavelength of a Bragg

resonance shifts with the sensor temperature. As the Bragg resonance minimum moves, the intensity decreases in channel λ_{k+1} , while it increases in channel λ_k . When a FBG sensor and an AWG both have approximately Gaussian passbands of comparable linewidths, the logarithmic ratio of the optical powers in channels λ_k and λ_{k+1} can be expressed as

$$\kappa(\delta\lambda) = \ln \frac{I_{k+1}}{I_k}, \quad (1)$$

where κ is a quasi-linear function of the wavelength [10], provided the FBG resonance wavelength shifts $\delta\lambda$ are small compared to the AWG channel spacing. Here I_k and I_{k+1} are the optical powers in channels λ_k and λ_{k+1} , respectively. The measured calibration logarithmic ratio κ is shown in Fig. 1b.

For the initial calibration of the system the TFBG was immersed in a temperature-controlled water bath. During the calibration the water temperature was gradually increased and each resonance wavelength shift $\delta\lambda$ was measured by the optical spectrum analyzer (OSA) as a function of the adjacent channel's intensity ratio measured by the microspectrometer, as shown in Fig. 1b. This calibration was carried out individually for the two (Bragg and cladding) resonances. The statistical deviation of the calibration measurements yields a wavelength resolution of 1.2 pm . The accuracy of the calibration instrument (OSA) is of the same order. This value is comparable to that achieved with complex and dedicated laboratory instruments such as OSAs and commercial wavelength swept laser interrogation systems [12].

The transmission spectrum of the TFBG is shown in Fig. 2. In our interrogation experiment a broadband Er^{3+} -doped fiber amplified spontaneous emission (ASE) source ($1530\text{--}1560 \text{ nm}$) was used as the light source. Since the TFBG cladding resonances as well as the nonuniform ASE emission spectrum extend over several FSRs of the AWG, the light source was prefiltered over two 1.5-nm -wide passbands centered near the Bragg core resonance (1546.2 nm) and one

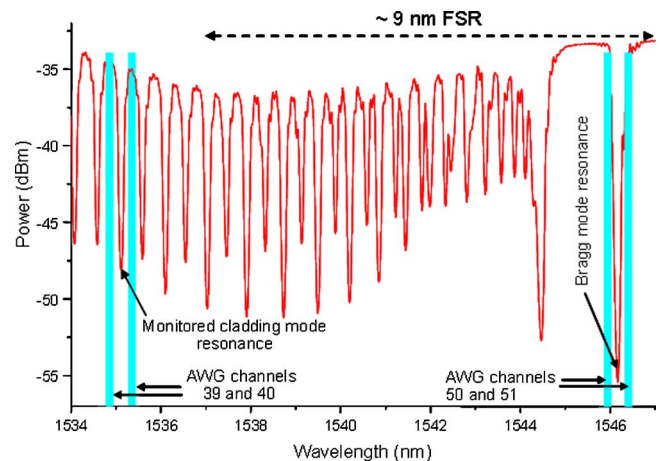


Fig. 2. (Color online) Measured TFBG transmission spectrum. The AWG channels used to monitor the cladding, and the Bragg mode resonances are indicated by the shaded areas.

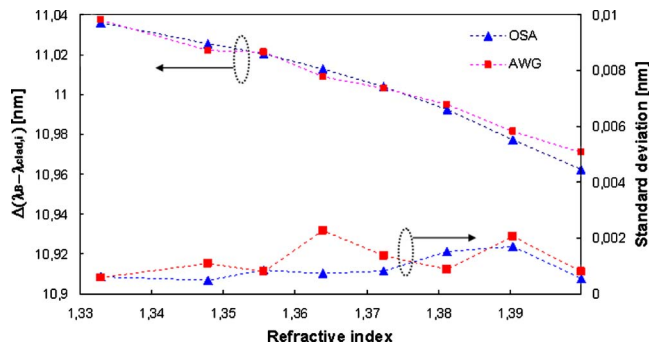


Fig. 3. (Color online) Measured differential wavelength shift between the cladding and the Bragg modes and the corresponding standard deviation data as a function of the sucrose solution refractive index.

of the cladding mode resonances (1535.2 nm), respectively. These two resonances are separated by more than one FSR, but since the light in between the two passbands from the source is blocked, both the Bragg and cladding resonances can be monitored simultaneously owing to the cyclic property of the AWG spectral response. This overlaying of the two FSRs allows the resonance of the cladding mode to be positioned between the channels 39 and 40, while the Bragg peak (11 nm from the cladding mode) is positioned between channels 50 and 51 (see Fig. 2). The light from the TFBG refractometric sensor is then coupled through a fiber splitter to the SOI AWG and an OSA. The OSA is used for calibrating the response of the SOI AWG and for comparative performance evaluation. The SOI AWG is temperature stabilized to $<0.1^\circ\text{C}$ at 23°C using a computer-controlled Peltier element. An image of the microspectrometer output waveguides 39/40 (cladding mode) and 50/51 (Bragg mode) is formed by a microscope objective on an infrared InGaAs camera. The relative intensity outputs from these four channels are extracted using a frame grabber and image analysis software.

For refractometric measurements, the TFBG was immersed in solutions of varying sucrose concentration, from 10% to 40% w/w in steps of 5% w/w (percents of total weight), corresponding to a refractive index step of 7.5×10^{-3} . The intensity ratios I_{k+1}/I_k were measured as a function of the sucrose solution refractive index [13] and the corresponding resonance wavelength shifts were obtained using the calibration data. The measurements were repeated ten times for each sucrose concentration over a period of 10 min. Figure 3 shows the measured differential wavelength shift $\Delta(\lambda_B - \lambda_{\text{clad},i})$ between the cladding and the Bragg modes and the corresponding standard deviation of the data at each sucrose concentration. Excellent agreement is observed between the interrogation results obtained using the OSA and the microspectrometer. The refractive index resolution is 1.2×10^{-3} , and it is limited by the specific type of TFBG we used in this experiment rather than by the interrogator itself. Various methods can be used to

increase the refractive index sensitivity of a FBG sensor. These include using a TFBG with a larger tilt angle, cladding modes near the cutoff condition, a thin high index coating overlayer, multiple cladding resonances within a single sensor measurement [11], and photonic wire evanescent field sensors [14].

We have reported an AWG interrogator device with a wavelength resolution of 1.2 pm comparable to that achieved with sophisticated and expensive spectroscopic instruments. Our interrogator is an integrated planar waveguide device with a compact footprint of $8 \text{ mm} \times 8 \text{ mm}$. By overlaying different AWG interference orders, the interrogator can simultaneously monitor widely separated resonances in real time with high wavelength resolution. Another important advantage of our SOI AWG interrogator is that it can be mass produced using established silicon-based microfabrication processes, which implies obvious cost benefits. Similar interrogator devices can be used for both well-established sensing applications including the monitoring of temperature, strain, pressure and microbending, and emerging applications such as chemical, biological, and environmental sensing.

This work was supported in part by the Genome and Health Initiative (GHI) program of the National Research Council of Canada (NRC).

References

1. M. K. Smit, *Electron. Lett.* **24**, 385 (1988).
2. C. Dragone, *J. Lightwave Technol.* **7**, 479 (1989).
3. C. Dragone, *IEEE Photon. Technol. Lett.* **3**, 812 (1991).
4. P. Cheben, in *Optical Waveguides: From Theory to Applied Technologies*, M. L. Calvo and V. Lakshminarayanan, eds. (CRC, 2007), Chap. 5.
5. P. Cheben, D.-X. Xu, S. Janz, and A. Del age, *Proc. SPIE* **5117**, 147 (2003).
6. P. Cheben, J. H. Schmid, A. Del age, A. Densmore, S. Janz, B. Lamontagne, J. Lapointe, E. Post, P. Waldron, and D.-X. Xu, *Opt. Express* **15**, 2299 (2007).
7. Y. Sano, N. Hirayama, and T. Yoshino, *Proc. SPIE* **4185**, 788 (2000).
8. P. Niewczas, A. J. Willshire, L. Dziuda, and J. R. McDonald, *IEEE Trans. Instrum. Meas.* **53**, 1192 (2004).
9. G. Z. Xiao, P. Zhao, F. G. Sun, Z. G. Lu, Z. Zhang, and C. P. Grover, *Opt. Lett.* **29**, 2222 (2004).
10. Y. Sano and T. Yoshino, *J. Lightwave Technol.* **21**, 132 (2003).
11. C.-F. Chan, C. Chen, A. Jafari, A. Laronche, D. J. Thomson, and J. Albert, *Appl. Opt.* **46**, 1142 (2007).
12. High resolution swept laser interrogator, Model Si720, from Micron Optics, Inc., Atlanta, Ga.
13. Reichert Analytical Instruments, <http://www.reichertai.com/files/applications/1039637372.PDF>.
14. D.-X. Xu, A. Densmore, P. Waldron, S. Janz, J. Lapointe, A. Del age, G. Lopinski, T. Mischki, P. Cheben, E. Post, and J. H. Schmid, and C. Storey, in *IEEE Lasers and Electro-Optics Society Annual Meeting Conference Proceedings* (IEEE, 2007), paper TuQ2.